10^{th} International Conference on Fracture Mechanics of Concrete and Concrete Structures
FraMCoS-X
G. Pijaudier-Cabot, P. Grassl and C. La Borderie (Eds)
https://doi.org/10.21012/FC10.233759

PHASE FIELD METHOD FOR MIROCRACKING SIMULATIONS IN CONCRETE MICROSTRUCTURE MODELS OBTAINED FROM 3D MICROTOMOGRAPHY IMAGES

J. YVONNET*, T.T. NGUYEN*, M. BORNERT†, C. CHATEAU†

*Université Paris-Est
5 bd Descartes, 77454 Marne-la-Vallée, France
Laboratoire Modélisation et Simulation Multi Echelle
e-mail: julien.yvonnet@univ-paris-est.fr

†Université Paris-Est
6/8 avenue Blaise Pascal, 77454 Marne-la-Vallée, France
Laboratoire Navier, ENPC, IFSTTAR e-mail: michel.bornert@enpc.fr

Key words: Crack propagation, phase field method, concrete, plaster, interfaces, micro-CT tomography.

Abstract. In this work, we present results obtained in our recent works regarding the simulation of 3D microcracks in concrete microstructures whose geometries are obtained by micro tomography images. The phase field method for quasi brittle fracture is employed to simulate the initiation, propagation and merging of microcracks networks. Using in-situ testing and micro tomography images of concrete microstructures, the initial microstructure geometries are used to simulate the full 3D crack network for direct validation with the experiments. The obtained predictability of the model allows developing inverse approaches to identify the microstructural damage parameters. Extensions of the phase field method to interfacial damage is proposed to predict the interaction between bulk micro crack networks with interfacial debounding, occurring at the sand grains and the cement paste interfaces. Examples of large scale simulations (involving up to 30 million voxels) of crack propagations are presented.

1 Introduction

Prediction of fracture resistance in civil engineering materials is a central and major issue in engineering. Achieving this objective through simulation modeling methods faces several technical and scientific obstacles. One possible way for constructing more predictable rupture models is to go down to the microstructure of the materials. However, such a strategy leads to several difficulties, including: (a) the development of crack propagation simulation methods in complex geometrical configurations associated with heterogeneous microstructures; (b) the construction of models for microstructural phenomena and their identification, whose coefficients can be hardly be accessed through common measurement methods; (c) constructing the macroscopic damage models from the microstructural models and (d) developing adapted experimental methods for exchanging information with the simulations.

In the present work, [8–12], we first propose to develop the modeling and simulation methods for the initiation and propagation of complex micro crack networks as found in concrete materials. Then, we combine these tools with microtomography images and in situ test to construct the microstructural models. Then, we develop identification and validation procedures combining the simulations and the experiments.

The crack propagation modeling and simulation method is based on the variational approach to fracture as proposed by Bourdin, Marigo and Francfort [4–6], and developed in an efficient algorithmic framework by Miehe et al. [7]. This method allows circumventing several well-known issues in fracture simulation and offer many advantages such as: (a) a simple numerical framework involving classical finite elements only; (b) mesh-independence; (c) the convergence with respect to the mesh size; (d) the possibility to handle initiation, propagation and merging of a large number of microcracks in 3D complex configurations; (e) a great numerical robustness and efficiency. We show that this technique is especially well adapted to the modeling of cracking in microstructural models directly obtained by images e.g. through micro-CT tomography, which form grids of voxels. We then present extensions of this technique for interfacial damage and interactions between bulk and interface cracks. Direct comparisons between 3D microcrack networks obtained by experiments and by simulations are provided.

2 The phase field method to fracture

The variational approach to fracture formulates the crack propagation problem as a minimization problem, where the energy of the cracked solid is expressed by:

$$E = \int_\Omega \Psi(\mathbf{u}, \Gamma) d\Omega + G_c \int_\Gamma d\Gamma \qquad (1)$$

where $\Psi(\mathbf{u}, \Gamma)$ is the strain density function depending on the displacement field and the crack network, collectively denoted by Γ, and G_c denotes the toughness in the sense of Griffith. The variational principle can be formulated as follows: for a given load, find the displacement field and the crak network Γ minimizing the energy, with a constraint of positive crack propagation rate. A direct use of this approach induces intractable numerical complications. To avoid this difficulty, a regularized approach of discontinuities description has been proposed, where the original function is replaced by an approximate one [1]. In this framework, the cracks are no more described by surfaces but by a field of damage pase $d(\mathbf{x})$. The energy is then expressed by:

$$E = \int_\Omega \Psi(\mathbf{u}, d) d\Omega + G_c \int_\Omega \gamma(d, \nabla d) d\Omega \qquad (2)$$

where γ is a function describing the crack density. The variational problem is here only related to variable fields, which avoids complex numerical techniques associated to remeshing crack surfaces. The variational problem can be formulated in a simpler framework by introducing a time discretization $T = \left\{t^0, t^1, ..., t^n, t^{n+1}, ..., t^N\right\}$. At each time step t^{n+1}, the problem relies on determining the displacement field $\mathbf{u}^{n+1}$ and the damage field d^{n+1} such that:

$$\mathbf{u}^{n+1}, d^{n+1} = \underset{\substack{\mathbf{u} \in \mathcal{K}_A \\ 0 \le d^n \le d^{n+1}}}{\text{Argmin}}\, E \qquad (3)$$

where $\mathcal{K}_A$ is a field of kinematically admissible displacements. Using a so-called first-order for the crack density function (see e.g. [7]):

$$\gamma(d, \nabla d) = \frac{1}{2\ell} d^2 + \frac{l}{2} \nabla d \cdot \nabla d, \qquad (4)$$

we obtain coupled problems to determine $d(\mathbf{x})$ and $\mathbf{u}(\mathbf{x})$, $\forall \mathbf{x} \in \Omega$ (see e.g. [7, 11]):

$$\begin{cases} 2(1-d)\mathcal{H} - \dfrac{g_c}{\ell}\left\{d - \ell^2 \Delta d\right\} = 0 \;\text{ in } \Omega, \\ d(\mathbf{x}) = 1 \;\text{ on } \Gamma, \\ \nabla d(\mathbf{x}) \cdot \mathbf{n} = 0 \;\text{ on } \partial\Omega, \end{cases} \qquad (5)$$

and

$$\begin{cases} \nabla \cdot \boldsymbol{\sigma}(\mathbf{u}, d) = \mathbf{f} \;\text{ in } \Omega, \\ \mathbf{u}(\mathbf{x}) = \overline{\mathbf{u}} \;\text{ on } \partial\Omega_u, \\ \boldsymbol{\sigma}\mathbf{n} = \overline{\mathbf{F}} \;\text{ on } \partial\Omega_F. \end{cases} \qquad (6)$$

In (4), ℓ is a regularization parameter related to crack width. A history function for the strain density function $\mathcal{H}(\mathbf{x}, t)$ is introduced, where t denotes time (or loading evolution in a quasi-static framework), to introduce the irreversibility of damage growth [7] and possible opening and closure of cracks:

$$\mathcal{H}(\mathbf{x},t) = \max_{\tau\in[0,t]} \left\{ \Psi^{+}\left(\mathbf{x},\tau\right) \right\}. \quad (7)$$

In (7), Ψ^{+} is the positive part of the strain density function such that: $\Psi = \Psi^{+}(\boldsymbol{\varepsilon}^{+}) + \Psi^{-}(\boldsymbol{\varepsilon}^{-})$ and is defined according to:

$$\Psi^{+}(\boldsymbol{\varepsilon}) = \frac{\lambda}{2}\left(\langle Tr(\boldsymbol{\varepsilon})\rangle_{+}\right)^{2} + \mu Tr\left\{\left(\boldsymbol{\varepsilon}^{+}\right)^{2}\right\}, \quad (8)$$

where $\boldsymbol{\varepsilon}$ is the linearized strain tensor, $\langle x\rangle_{\pm} = (x \pm |x|)/2$ and $\boldsymbol{\varepsilon}^{\pm}$ denote positive and negative parts of the strain tensor (see [7, 11]). The choice of the parameter ℓ has been discussed in [2, 3, 10, 13].

In (6), $\boldsymbol{\sigma} = \frac{\partial W}{\partial \boldsymbol{\varepsilon}}$ is the Cauchy stress tensor, $\mathbf{f}$ is a body forces vector and $\overline{\mathbf{u}}$ et $\overline{\mathbf{F}}$ are prescribed displacement and force on the related boundaries $\partial\Omega_u$ and $\partial\Omega_F$, respectively. Above, $\nabla(.)$ and $\nabla\cdot(.)$ denote gradient and divergence operators. For the strain density function (8), the constitutive law is obtained as [7]:

$$\boldsymbol{\sigma} = \left((1-d)^2 + k\right)\left\{\lambda\langle Tr\boldsymbol{\varepsilon}\rangle_{+}\mathbf{1} + 2\mu\boldsymbol{\varepsilon}^{+}\right\}$$

$$+ \lambda\langle Tr\boldsymbol{\varepsilon}\rangle_{-}\mathbf{1} + 2\mu\boldsymbol{\varepsilon}^{-} \quad (9)$$

where $k << 1$ is a positive scalar parameter introduced to avoid loss of stability in fully damaged elements. Eqs. (5)-(6) are solved by a classical finite element method at each time stem (load increment).

3 Extension of the phase field method to interfacial damage

In this part, we present an extension of the phase field method to interfacial damage as proposed in [12], this type of mechanism being especially important in concrete materials.

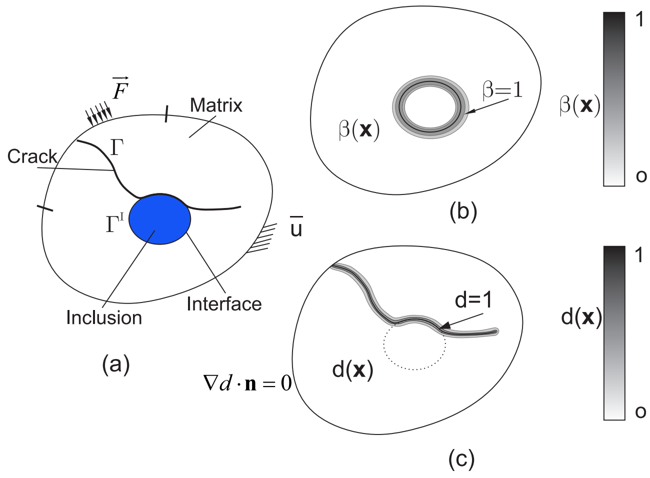

Figure 1: Regularized representation of a crack and of an interface: (a) solid containing an interface and a crack, with possible propagation of the bulk crack in the interfaces; (b) regularized representation of an interface; (c) regularized representation of a crack.

We consider here a set of interfaces between the inclusions and the matrix, denoted collectively by Γ^I. During loading, cracks can propagate in the matrix but can also propagate within the interfaces, as depicted in Fig. 1(a). Regularization of interfacial discontinuities is performed according to the framework proposed in [12]. Both bulk and interfacial cracks are associated with the field $d(\mathbf{x},t)$ (see Fig. 1(c)), while regularized interface indicators are associated with a fixed scalar field $\beta(\mathbf{x})$ (see Fig. 1(b)) only employed to represent geometrically the interfaces in regular grids of voxel type, and which satisfies:

$$\begin{cases} \beta(\mathbf{x}) - \ell_\beta^2(\mathbf{x})\triangle\beta(\mathbf{x}) = 0 \ \text{ in } \Omega, \\ \beta(\mathbf{x}) = 1 \ \text{ on } \Gamma^I, \\ \nabla\beta(\mathbf{x})\cdot\mathbf{n} = 0 \ \text{ on } \partial\Omega, \end{cases} \quad (10)$$

where ℓ_β is a regularization parameter for the interfaces. The variational principle (3) is extended by including the presence of interfaces and of a different associated behavior by modifying the expression of the energy as:

$$E = \int_\Omega \Psi^e\left(\boldsymbol{\varepsilon}^e(\mathbf{u},\beta), d\right) d\Omega$$

$$+\int_{\Omega}[1-\beta(\mathbf{x})]g_c\gamma_d(d)d\Omega+\int_{\Omega}\Psi^I\gamma_\beta(\beta)d\Omega. \tag{11}$$

In (11) Ψ^I is a strain density function depending on a displacement jump across the interface Γ^I. In the context of regularized discontinuities, the strain field can be decomposed according to:

$$\boldsymbol{\varepsilon}=\boldsymbol{\varepsilon}^e+\tilde{\boldsymbol{\varepsilon}}, \tag{12}$$

where $\boldsymbol{\varepsilon}^e$ is the strain part associated to the bulk and $\tilde{\boldsymbol{\varepsilon}}$ represents the part of the strain induced by the regularized displacement jump and where [12]:

$$\tilde{\boldsymbol{\varepsilon}}=\frac{1}{2}\left(\mathbf{n}\otimes[[\mathbf{u}]]+[[\mathbf{u}]]\otimes\mathbf{n}\right)\gamma_\beta(\mathbf{x}). \tag{13}$$

This decomposition is proposed such that $\tilde{\boldsymbol{\varepsilon}}\rightarrow 0$ away from the interfaces, inducing $\beta(\mathbf{x})\rightarrow 0$. The term $[1-\beta(\mathbf{x})]$ is introduced to verify that when $\beta(\mathbf{x})\rightarrow 0$ (away from the interfaces), then $\gamma_\beta\rightarrow 0$ and $\boldsymbol{\varepsilon}^e\rightarrow\boldsymbol{\varepsilon}$. A definition for the regularized displacement jump can be found in [12].

4 Applications to microstructures of cementitious materials

We propose here some applications of microcracking simulations and comparisons with in-situ testing experiments combined with micro-CT images. In Fig. 2, we consider a sample of lightweight concrete (containing PE beads). The microtomography allows obtaining a full 3D representation of the sample microstructure geometry (after a treatment of the grey-level images and segmentation procedure). The initial model can then be used to simulate the initiation and propagation of microcracks by using the above phase field framework.

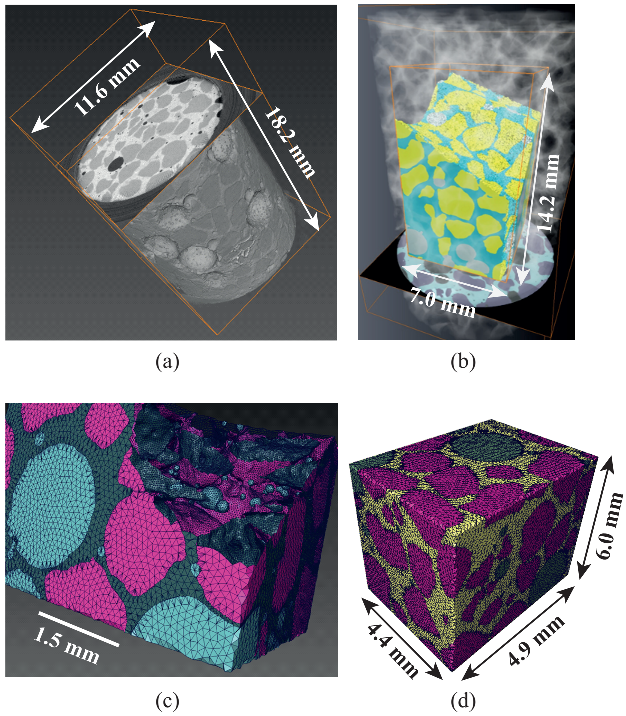

Figure 2: (a) Full image obtained by micro-CT scan of a lightweight concrete sample: (b)-(c)-(d) show different view of the associated mesh containing 17M elements.

A mesh is then constructed from the segmented image, either by associating directly each voxel to a finite element in a regular mesh (which limits the size of the considered zone), or by reconstructing the interfaces and remeshing the constructed geometry (unstructured mesh). This last technique allows refining and coarsening some areas to limit the number of elements and to analyze larger domains within the segmented image. In Fig. 3, an example of comparison between simulation and experiment is presented. The external boundary conditions applied on the boundary of the numerical model are obtained from experimental 3D image correlation. We can observe that the simulations provide a very good prediction as compared to experiments. it is also noteworthy that the local (microstructural) damage parameters have been identified by an inverse approach analysis (see [8]).

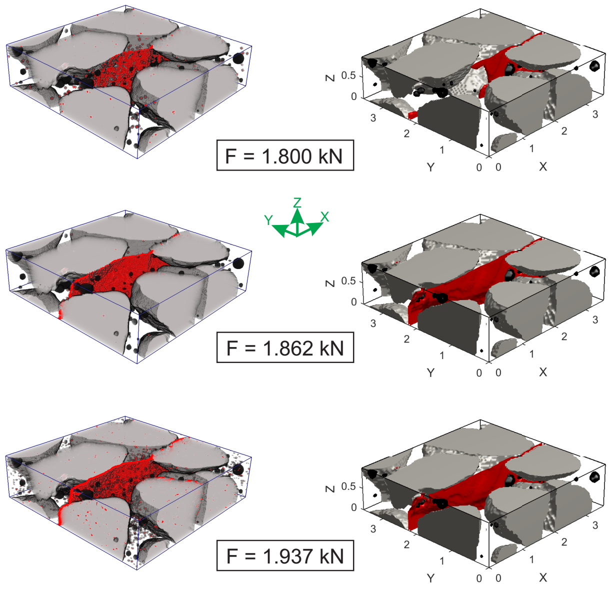

Figure 3: Comparisons between cracks obtained from experiments and by in-situ experimental test in a lightweight concrete: (Left: experiments; right: numerical simulations by phase field method).

Another example of such comparison is provided in fig. 4. Here we consider a sample of lightweight plaster (plaster matrix with PE inclusions). The geometry is here simpler and allows considering the whole sample. We can here again note the very good predictability of the simulation, which allows to capture a large number of cracks observed in the simulation.

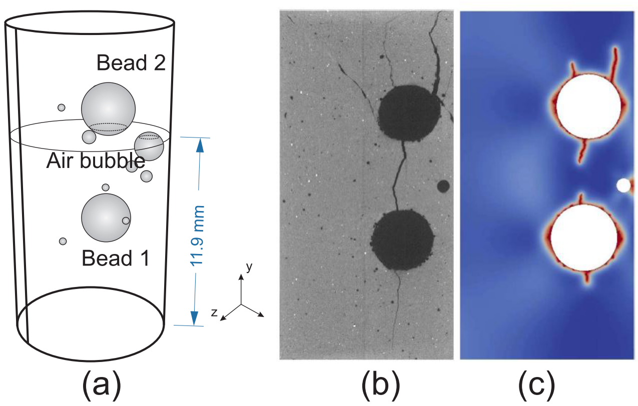

Figure 4: (a) Geometry of the lightweight plaster sample; -b) experimental cracks; (c) cracks obtained by the numerical simulations (for the same applied load $F = 2.64$ kN) [9].

REFERENCES

[1] L. Ambrosio and V. Tortorelli. Approximation of functionals depending on jumps by elliptic functionals via Γ-convergence. *Comm. Pure Appl. Math.*, 43:999–1036, 1990.

[2] H. Amor, J.-J. Marigo, and C. Maurini. Regularized formulation of the variational brittle fracture with unilateral contact: Numerical experiments. *Journal of the Mechanics and Physics of Solids*, 57(8):1209–1229, 2009.

[3] M. Borden, C. Verhoosel, M. Scott, T. Hughes, and C. Landis. A phase-field description of dynamic brittle fracture. *Computer Methods in Applied Mechanics and Engineering*, 217:77–95, 2012.

[4] B. Bourdin, G. Francfort, and J. Marigo. Numerical experiments in revisited brittle fracture. *Journal of the Mechanics ad Physics of Solids*, 48:797–826, 2000.

[5] B. Bourdin, G. Francfort, and J. Marigo. *The Variational Approach to Fracture*. Springer-Verlag, Berlin, 2008.

[6] G. Francfort and J. Marigo. Revisiting brittle fracture as an energy minimization problem. *Journal of the Mechanics and Physics of Solids*, 46(8):1319–1342, 1998.

[7] C. Miehe, M. Hofacker, and F. Welschinger. A phase field model for rate-independent crack propagation: Robust algorithmic implementation based on operator splits. *Computer Methods in Applied Mechanics and Engineering*, 199:2776–2778, 2010.

[8] T. Nguyen, J. Yvonnet, M. Bornert, and C. Chateau. Direct comparisons of 3D crack networks propagation in cementitious materials between phase field numerical modeling and in-situ microtomography experimental images. *Journal of the Mechanics and Physics of Solids*, 95:320–350, 2016.

[9] T. Nguyen, J. Yvonnet, M. Bornert, C. Chateau, F. Bilteryst, and E. Steib. Large-scale simulations of quasi-brittle microcracking in realistic highly heterogeneous microstructures obtained from micro ct imaging. *Extreme mechanics letters*, 17:50–55, 2017.

[10] T. Nguyen, J. Yvonnet, M. Bornert, C. Chateau, K. Sab, R. Romani, and R. L. Roy. On the choice of parameters in the phase field method for simulating crack initiation with experimental validation. *Int. J. Fract.*, 197(2):213–226, 2016.

[11] T. Nguyen, J. Yvonnet, Q.-Z. Zhu, M. Bornert, and C. Chateau. A phase field method to simulate crack nucleation and propagation in strongly heterogeneous materials from direct imaging of their microstructure. *Engineering Fracture Mechanics*, 139:18–39, 2015.

[12] T. Nguyen, J. Yvonnet, Q.-Z. Zhu, M. Bornert, and C. Chateau. A phase-field method for computational modeling of interfacial damage interacting with crack propagation in realistic microstructures obtained by microtomography. *Computer Methods in Applied Mechanics and Engineering*, (312):567–595, 2016.

[13] K. Pham, J.-J. Marigo, and C. Maurini. The issues of the uniqueness and the stability of the homogeneous response in uniaxial tests with gradient damage models. *Journal of the Mechanics and Physics of Solids*, (6), 2011.